Supplement of Atmos. Chem. Phys., 16, 13823–13836, 2016
http://www.atmos-chem-phys.net/16/13823/2016/
doi:10.5194/acp-16-13823-2016-supplement

Atmospheric Chemistry and Physics Open Access EGU

Supplement of

Single-particle investigation of summertime and wintertime Antarctic sea spray aerosols using low-*Z* particle EPMA, Raman microspectrometry, and ATR-FTIR imaging techniques

Hyo-Jin Eom et al.

Correspondence to: Chul-Un Ro (curo@inha.ac.kr)

Table S1. Average elemental concentrations of individual particles in summertime and wintertime $PM_{2.5-10}$ and $PM_{1.0-2.5}$ fractions using low-*Z* particle EPMA.

sample	Summertime sample S1				Wintertime sample S2			
size fraction	$PM_{1.0-2.5}$ (stage 3)		$PM_{2.5-10}$ (stage 2)		$PM_{1.0-2.5}$ (stage 3)		$PM_{2.5-10}$ (stage 2)	
number of particles	146		148		154		156	
average size (μm)	2.0 (±0.6)		2.9 (±1.5)		1.7 (±0.8)		3.2 (±1.5)	
element	at. conc. (%)	wt. conc. (%)	at. conc. (%)	wt. conc. (%)	at. conc. (%)	wt. conc. (%)	at. conc. (%)	wt. conc. (%)
C	27.1 (±4.8)	14.6	21.9 (±5.9)	11.5	21.6 (±5.1)	11.2	18.8 (±3.8)	9.6
O	17.3 (±3.2)	12.4	19.5 (±4.7)	13.6	17.4 (±3.2)	12.0	18.2 (±4.0)	12.3
Na	25.2 (±3.3)	25.9	26.1 (±3.4)	26.2	27.6 (±4.2)	27.3	28.3 (±4.0)	27.5
Mg	2.3 (±0.4)	2.5	2.7 (±0.7)	2.9	2.9 (±0.5)	3.0	2.7 (±0.6)	2.8
Si	0.8 (±0.5)	1.0	0.3 (±0.4)	0.4	0.0	0.0	0.0	0.0
S	1.6 (±0.3)	2.3	1.8 (±0.5)	2.5	1.6 (±0.2)	2.2	1.6 (±0.3)	2.2
Cl	24.8 (±3.7)	39.4	26.4 (±3.4)	40.9	28.1 (±4.1)	42.8	29.2 (±3.8)	43.8
K	0.5 (±0.2)	0.9	0.5 (±0.2)	0.9	0.4 (±0.3)	0.7	0.5 (±0.2)	0.8
Ca	0.6 (±0.2)	1.1	0.7 (±0.3)	1.2	0.5 (±0.6)	0.9	0.6 (±0.3)	1.0

Figure S1. Three-day (72 h) backward air mass trajectories at 500 m-, 1000 m- and 1500 m-receptor heights in December 9, 2011 and July 23, 2012. HYbrid Lagrangian Single-Particle Integrated Trajectory (HYSPLIT) model available at the NOAA Air Resources Laboratory's web server (http: //www.arl.noaa.gov/ready/hysplit4.html) was used.

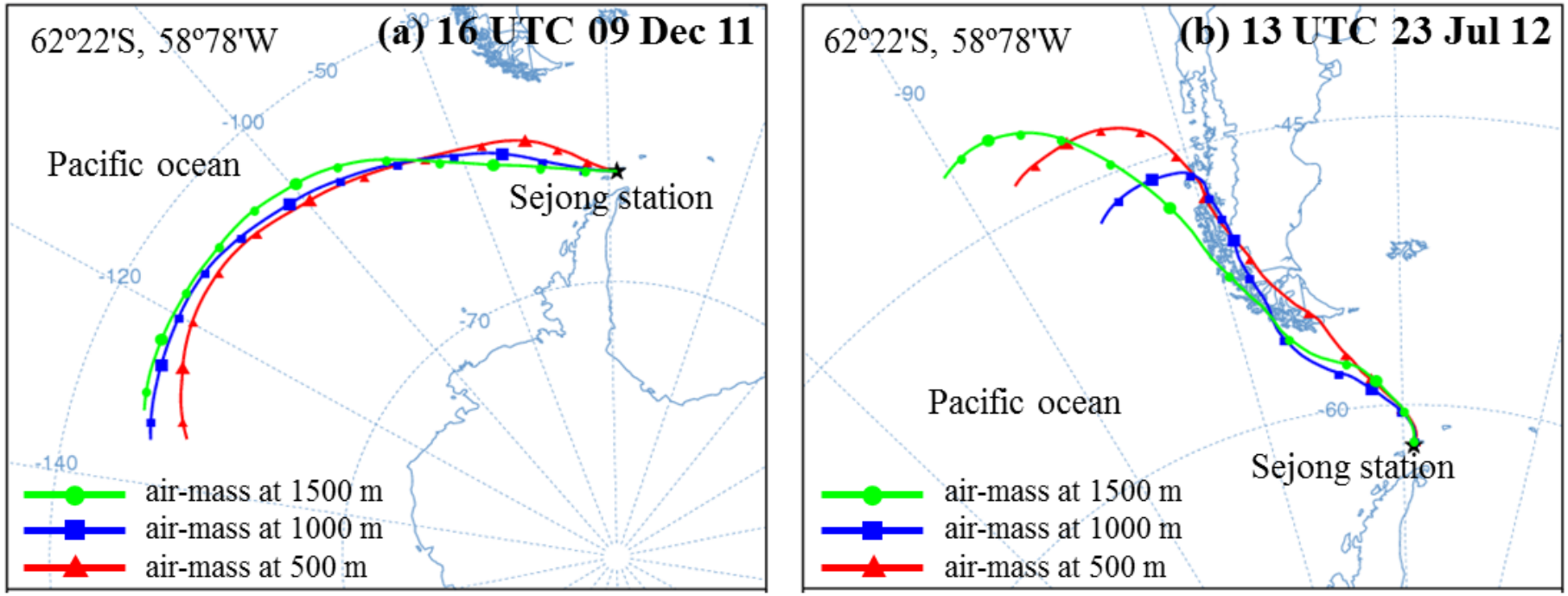

Figure S2. Relative abundances of individual particles in two size fractions of the summer and winter samples, having specific concentration ratios of (a) C, (b) S, (c) Ca, (d) Cl, (e) Mg, and (f) K to Na. The red solid and dotted lines demote the stage 2 ($PM_{2.5\text{-}10}$) and stage 3 ($PM_{1.0\text{-}2.5}$) particles of the summertime sample, respectively, and the blue solid and dotted lines are for stage 2 ($PM_{2.5\text{-}10}$) and stage 3 ($PM_{1.0\text{-}2.5}$) particles of the wintertime sample, respectively. The green lines indicate bulk sea-water ratios corresponding to the elements.

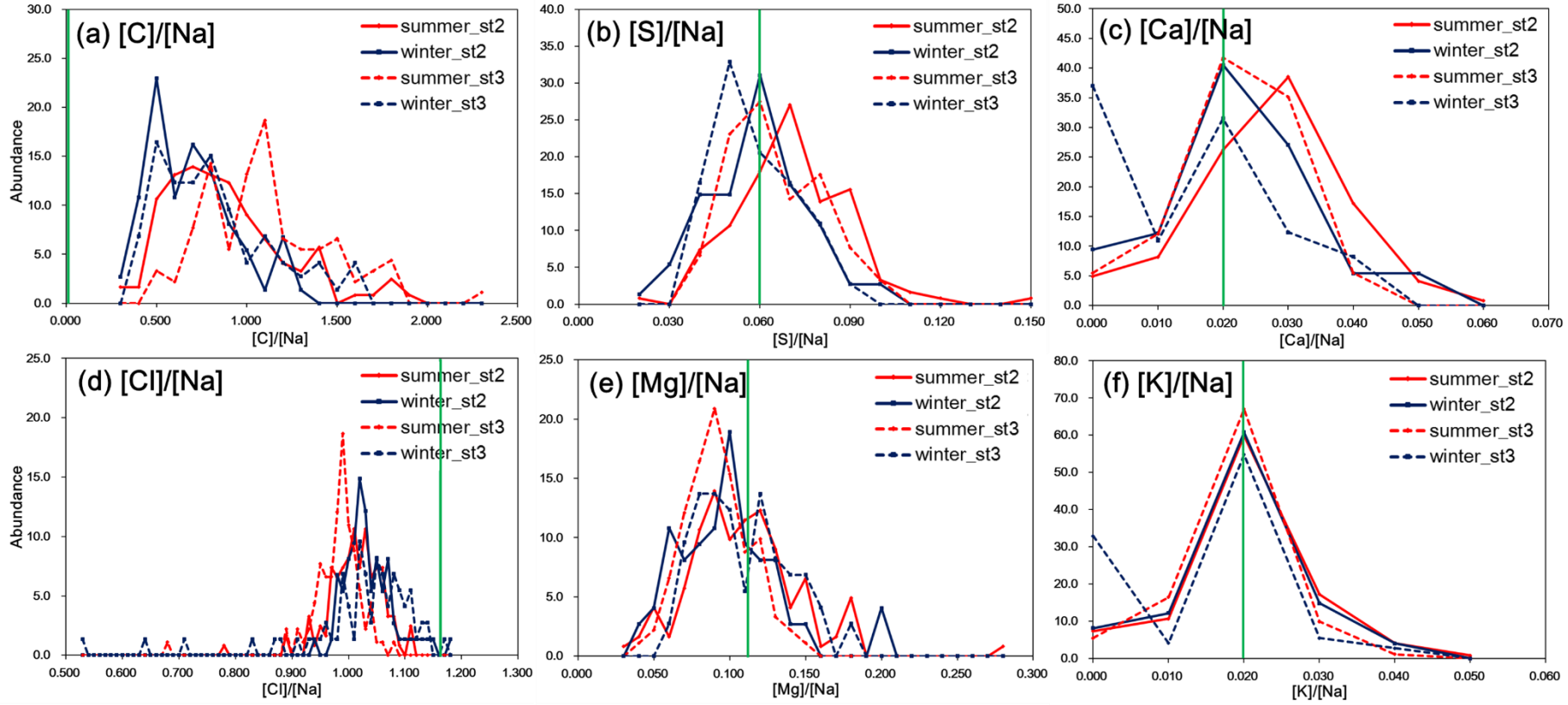

Figure S3. Raman and ATR-FTIR spectra of the aerosols generated by the nebulization of a mixture solution of 0.2 M alanine and 0.1 M $MgCl_2$ standard chemicals. The first pair of Raman and ATR-FTIR spectra for the aerosols was obtained just after the nebulization and the second and third pairs of Raman and ATR-FTIR spectra were obtained ~1 year later after the storage in a desiccator. The first and third pairs of Raman and ATR-FTIR spectra for organic moiety look similar to those in Figures 4(b) and 4(a), respectively.

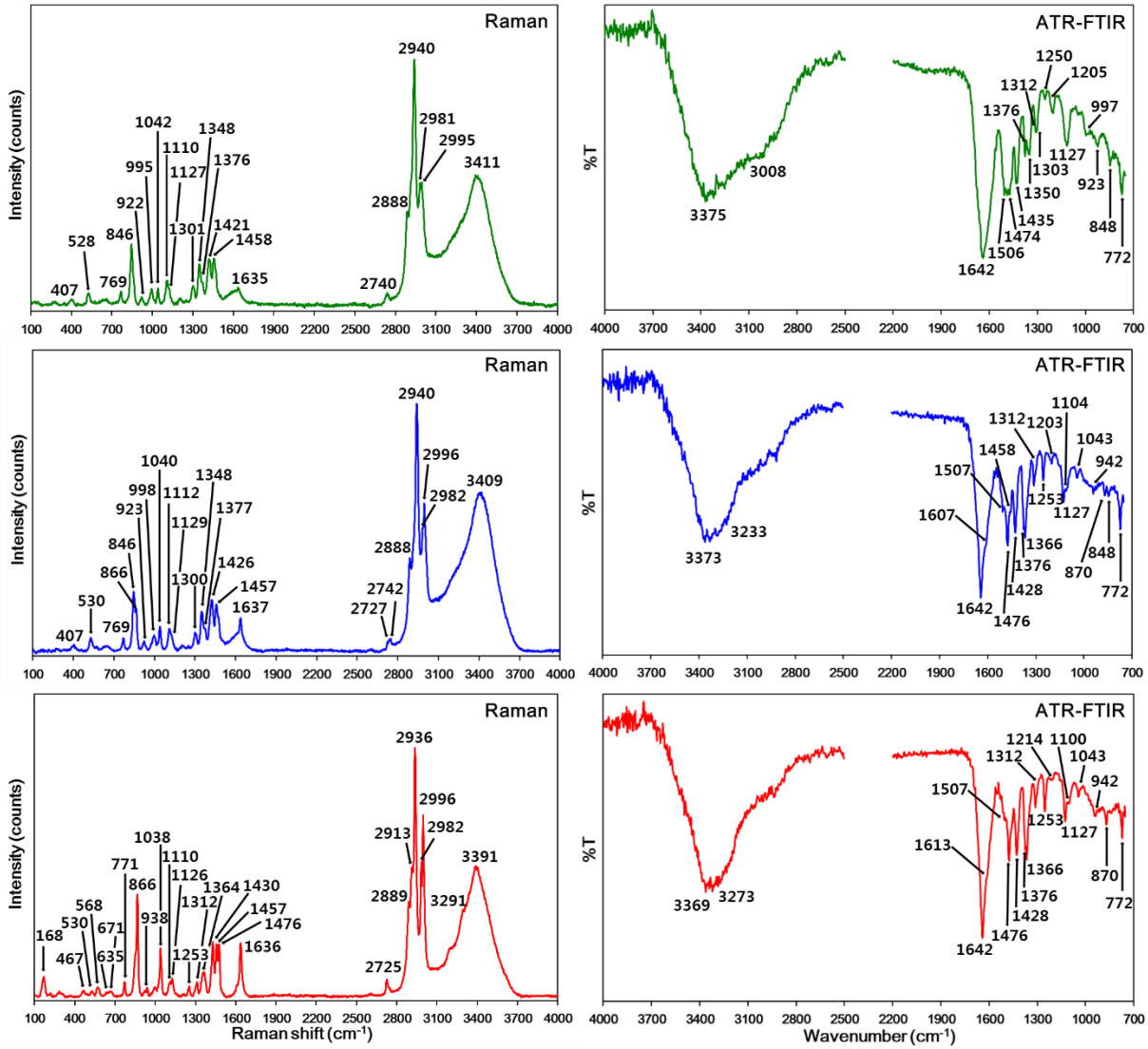

Figure S4. Raman and ATR-FTIR spectra of some target chemicals for organics in Antarctic SSAs, which do not resemble with those for MgAla-containing SSAs.

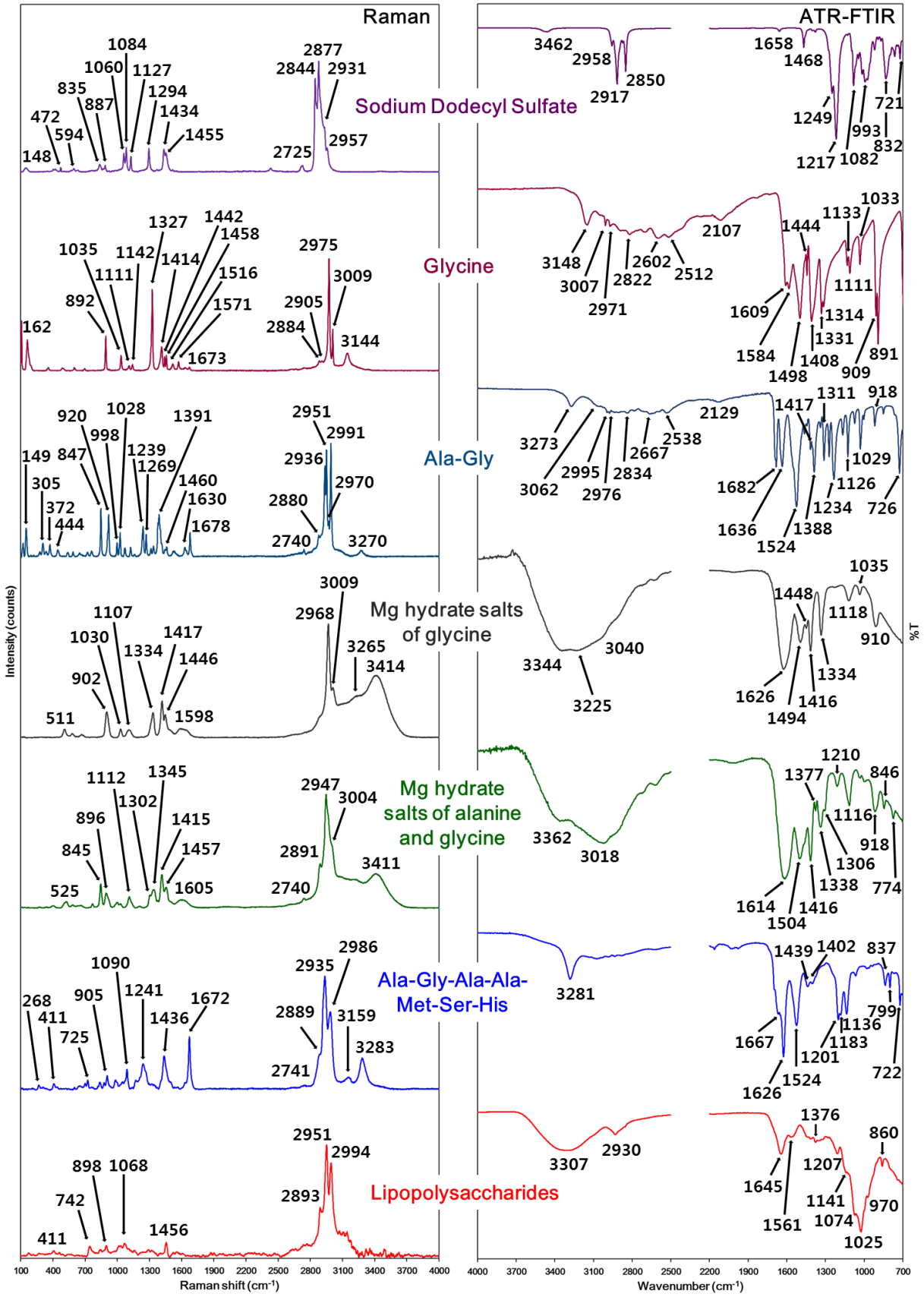

Figure S5. Raman and ATR-FTIR spectra of powdery standard Mg palmitate, palmitic acid, Mg stearate, and stearic acid, which are sufficiently different to distinguish the four compounds.

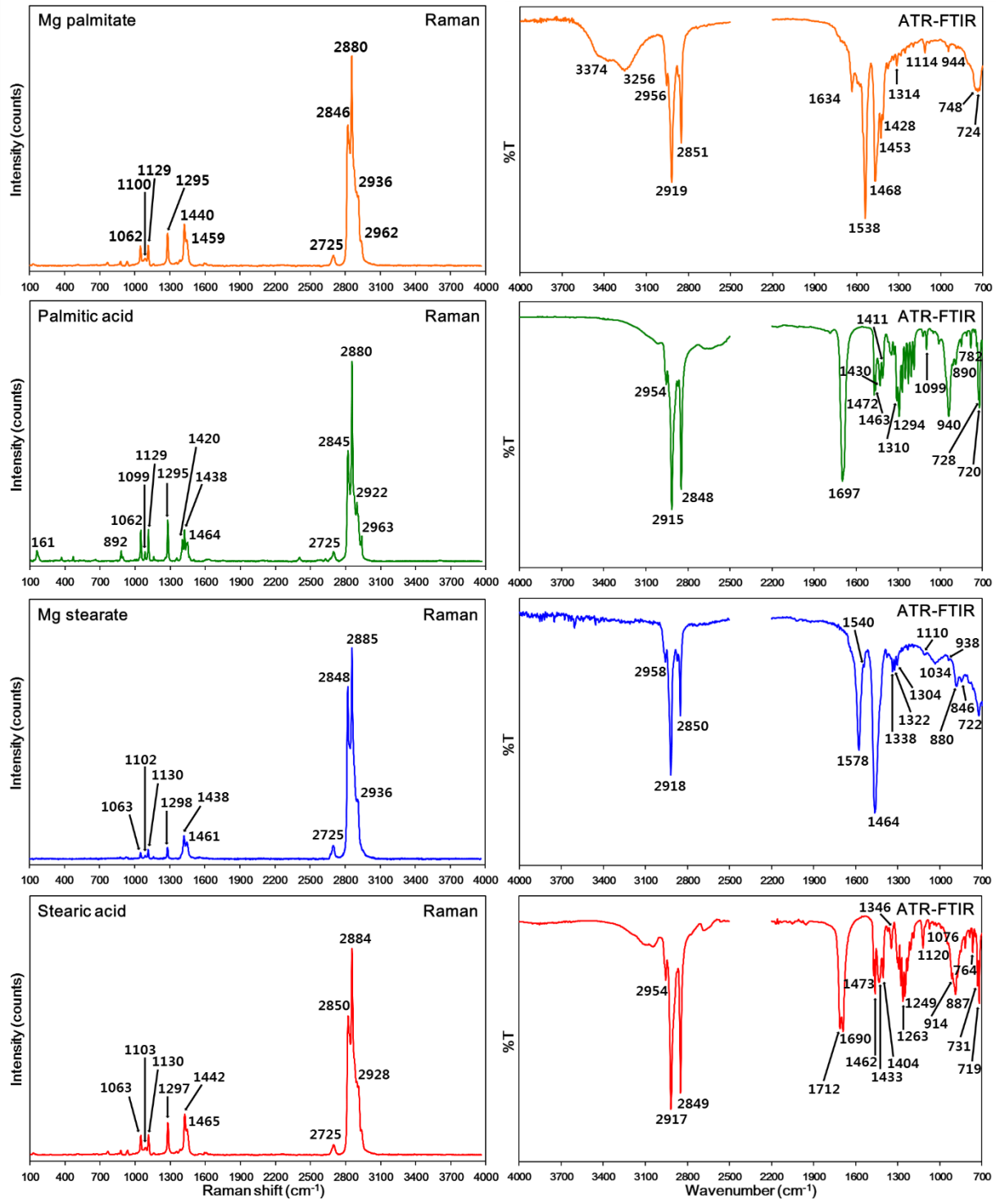

Figure S6. ATR-FTIR spectra of Mg palmitate, Mg stearate, a mixture of Mg palmitate and stearate (by 3:1), and MgFAs-containing SSA, showing that MgFAs-containing SSAs are the mixture of mainly Mg palmitate and stearate.

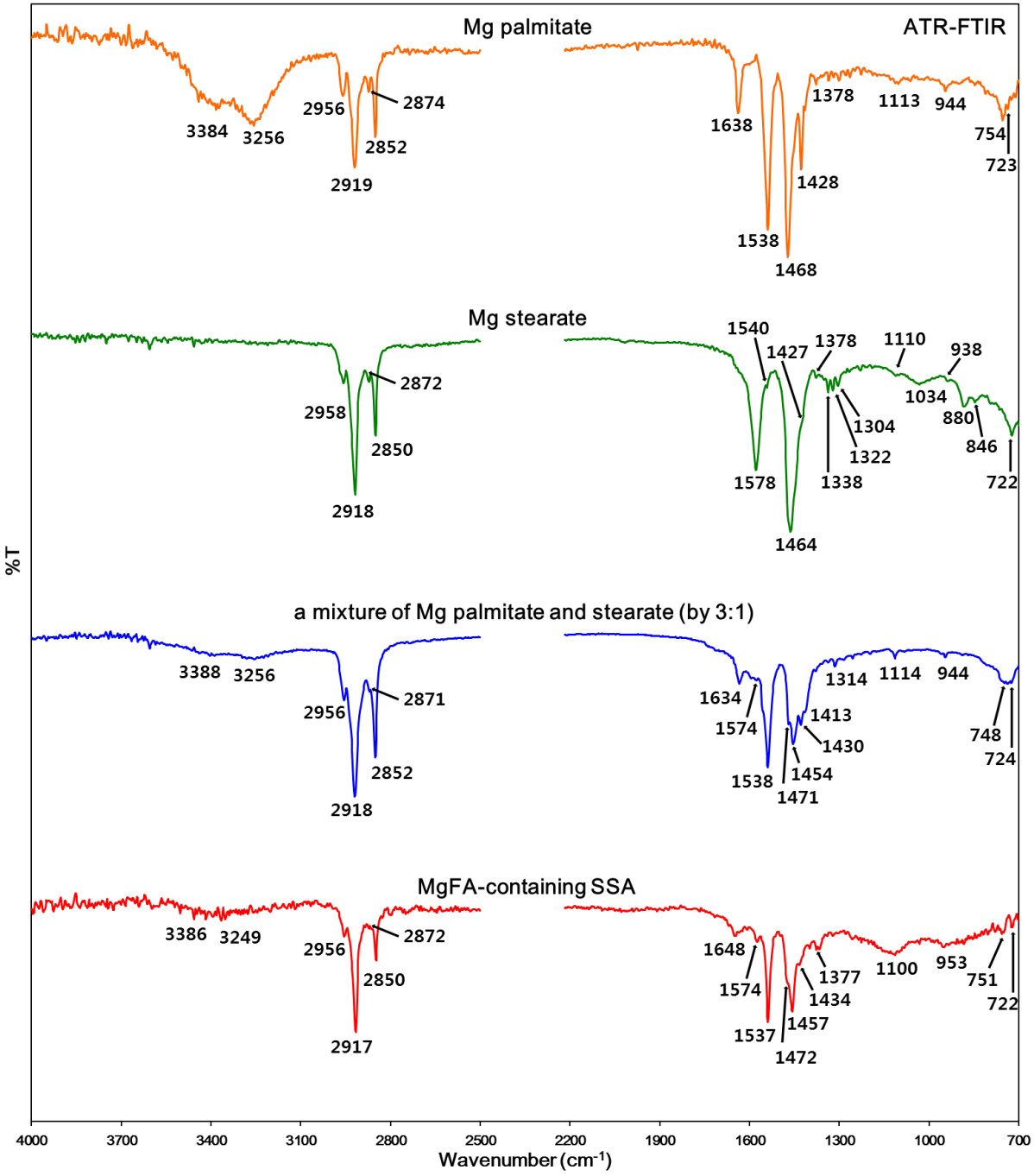

Figure S7. Raman and ATR-FTIR spectra of standard inorganic chemicals, which are observed in Antarctic SSAs.